# Determination of the first satellite valley energy in the conduction band of wurtzite GaN by near-band-gap photoemission spectroscopy

Marco Piccardo,[1,2] Lucio Martinelli,[1,*] Justin Iveland,[2] Nathan Young,[2] Steven P. DenBaars,[2] Shuji Nakamura,[2] James S. Speck,[2] Claude Weisbuch,[1,2] and Jacques Peretti[1]

[1]*Laboratoire de Physique de la Matière Condensée, CNRS–Ecole Polytechnique, Palaiseau, France*

[2]*Materials Department, University of California, Santa Barbara, California 93106, USA*

(Received 15 February 2014; revised manuscript received 5 June 2014; published 23 June 2014)

The position of the first satellite valley in wurtzite GaN is directly determined by near-band-gap photoemission spectroscopy of *p*-doped GaN activated to negative electron affinity. The photoemission spectra exhibit two structures, with fixed energy position, which originate from electrons accumulated in the conduction band valleys of the bulk material. We assigned the two observed features respectively to Γ and L valleys and obtain an intervalley energy separation of $0.90 \pm 0.08$ eV, well below the theoretical values of the lowest subsidiary valley energy provided by *ab initio* calculations.

DOI: 10.1103/PhysRevB.89.235124 PACS number(s): 71.20.Nr, 79.60.Bm

GaN and related wide-band-gap III-N semiconductor compounds play an ever increasing role in optoelectronics [1] and power electronics [2,3]. However, some of the fundamental properties of GaN are still poorly known despite the rapid progress in GaN-based technologies. In particular, the energy position of the satellite valleys of the conduction band (CB) is still debated while hot-electron transport is known to involve multivalley processes. Indeed, due to large internal electric fields, high-energy optical transitions, or Auger recombinations, conduction electrons may gain large kinetic energies and access higher minima of the CB by mean of phonon-assisted intervalley transfer. The upper valleys thus act as high-energy channels for electron transport.

The values of the first satellite valley position reported in the literature are scattered on a considerable range of about 2 eV. Several experimental determinations have been deduced from indirect measurements. Very low values of 340 meV and 290 meV above the CB minimum were deduced respectively from BEEM measurements [4] and from photoluminescence spectroscopy [5]. Other experimental determinations provide significantly larger values. Intervalley energy separation of ∼1.2 eV was obtained from photoexcited field emission on GaN nanorods [6]. Similar values are provided by pump-probe transient optical spectroscopy. Sun *et al.* [7] obtained a side-valley energy position of 1.34 eV in *n*-GaN. More recently Wu *et al.* [8] measured a $\Gamma \rightarrow$ L intervalley transfer onset occurring at an interband excitation energy of 4.51 eV which corresponds to an L-valley energy of ∼0.85 eV above the CB minimum when assuming parabolic bands with effective masses of $m_e^* = 0.22m_0$ and $m_{hh,z}^* = 1.58m_0$ for electrons [9,10] and holes [11], respectively, and taking $\hbar\omega_{iv} = 92$ meV as the intervalley phonon energy [12]. Finally, recent measurements of electron emission spectroscopy from a GaN light-emitting diode exhibit two electron peaks separated by $0.95 \pm 0.1$ eV attributed to Auger electrons scattered and accumulated in Γ and L valleys before emission in vacuum [13]. Much larger values are provided by *ab initio* band structure calculations. Wang *et al.* [14] predicted an energy position of 1.49 eV above the CB minimum for the first satellite valley [15]. More recently Goano *et al.* [16] and Delaney *et al.* [17] predicted a value of 2.25 eV, and De Carvalho *et al.* [18] obtained 2.06 eV. Thus, in the absence of a direct experimental determination, the position of the first satellite valley remains controversial.

A direct experimental access to the CB structure of semiconductors is provided by near-band-gap photoemission spectroscopy of negative electron affinity (NEA) photocathodes. Contrarily to the usual x-ray and UV photoemission spectroscopies techniques, near-band-gap photoemission of NEA semiconductors is mainly sensitive to the empty states structure. Indeed, it can be considered that the optical excitation creates $\delta$ distributions at well-defined energies in the conduction band corresponding to heavy-hole, light-hole, and spin-orbit split-off band. Then, electrons relax their energies by phonons scattering and a broad electron distribution forms, the detailed shape of which is determined by the hot-electron transport mechanisms in the conduction band. Therefore, the photoemitted electron spectrum contains very little information on the initial state of the optical transition. At best very weak structures corresponding to the final state of the optical transitions from the three valence bands are sometimes observed but not in the case of GaN, except for the high-energy threshold of the spectrum which is characteristic of the final state of the optical transition from the heavy-hole band. When varying the excitation energy $h\nu$, the features which show up in the energy distribution curves (EDCs) of the emitted photoelectrons can be unambiguously assigned either to the optical transition final states (allowing band dispersion measurement) or to the emission from side valleys at the bottom of which electrons accumulate during the relaxation process [19–21]. We here report on the experimental study of the CB structure of wurtzite *p*-GaN by near-band-gap photoemission spectroscopy for excitation energies ranging from 3.10 eV to 5.39 eV. In this energy range, two features associated with CB valleys are evidenced that we attribute to the Γ valley and to the first satellite valley (presumably L). We directly obtain the Γ-L intervalley energy separation of $0.90 \pm 0.08$ eV above the bottom of the conduction band, much lower than theoretical ones and in agreement with those recently estimated from optical spectroscopy experiments.

*lucio.martinelli@polytechnique.edu

 

The sample is a wurtzite GaN $p$-$n$ structure grown by metalorganic chemical vapor deposition on a (0001) sapphire substrate. The top $p$ layer is 200 nm thick, larger than the absorption length varying approximately from 110 nm down to 45 nm in the actual spectral range of above-band-gap excitation energies [22]. The acceptor (Mg) concentration is of $5 \times 10^{19}$ cm$^{-3}$ in the bulk and overdoped in the proximity of the surface. In this doping condition the width of the band-bending region (BBR) near the $p$ surface is less than 10 nm. The sample was chemically cleaned in a piranha solution and an HCl-isopropanol solution [23]. It was then introduced into the ultrahigh-vacuum chamber where the typical base pressure is in the low $10^{-11}$ Torr range. Details on the experimental setup and procedure are given elsewhere [24]. After annealing at 580 °C for ∼90 min, the $p$-GaN surface was activated to effective NEA by Cs deposition. The surface activation was controlled by monitoring the PE current under laser light excitation at $h\nu = 3.32$ eV. The cesiation procedure is completed when the quantum yield reaches a maximum value (typically 0.4%). In this condition, the work function is lowered to about 2.3 eV and remains stable for few days. The photoemission spectroscopy measurements were performed with a tunable light source (Energetiq EQ-99) coupled to a monochromator (Jobin-Yvon H10-UV) with an output wavelength bandwidth of ±2 nm. The light beam was focused at normal incidence on the $p$-GaN surface. Photoemitted electrons were analyzed with a low-energy electron spectrometer [13,25] which consists of a double electrostatic cylindrical 90° deflector working in constant path energy mode. In this operating mode the potentials of the electrodes are kept constant which defines the path energy $E_{\rm sel}$ and the resolution. The electrons of energy $E$ referred to the GaN Fermi level ($E_F$) pass through the analyzer and are collected on the Faraday cup when the potential $V_{\rm cath}$ applied to the sample satisfies to $E + qV_{\rm cath} = E_{\rm sel}$. The EDCs are then obtained by recording the Faraday cup current as a function of $V_{\rm cath}$. For the present study, the sample potential $V_{\rm cath}$ was applied on a gold contact evaporated on the $p$-GaN surface away from the photoexcited area. The resolution was set at 80 meV and the path energy $E_{\rm sel} = 4.62 \pm 0.02$ eV was determined by a calibration on the photoemission spectrum from the Fermi distribution of a gold sample.

Figure 1 shows schematics of the photoemission processes. Direct interband transitions excite electrons with a well-defined conduction energy. A small fraction of the photoelectrons are emitted without energy loss, yielding a quasiballistic hot-electron contribution (labeled B). This contribution extends up to the highest possible transition final state energy (related to transitions from the heavy-hole valence band) which defines the high-energy threshold of the photoemission EDCs. Most of the photoelectrons undergo energy and momentum relaxation by phonon emission. In the bulk, relaxation produces electron accumulation at the bottom of the conduction valleys. For moderate light energy above the band gap, electrons are photoexcited in the Γ valley but if the transition final state energy lies above a satellite valley minimum, electrons can be efficiently transferred from Γ to the satellite valley by emitting a phonon. We remark that the L valley in wurtzite crystals has a sixfold degeneracy giving a large final density of states for intervalley transfers. Each populated valley acts as a source of thermalized electrons.

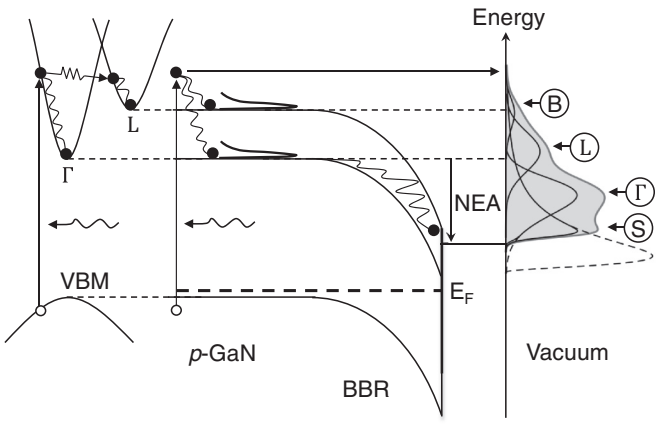


FIG. 1. Left: Reciprocal-space schematic of photoelectron excitation and intervalley transfer from Γ to L valley via phonon emission. Right: Real-space schematic of the photoemission processes occurring in $p$-GaN at above-band-gap excitation. Quasiballistic electron emission produces a high-energy peak (labeled B). Energy relaxation induces electron accumulation in the bulk at the bottom of the conduction band valleys (peaks Γ and L). Relaxation in the BBR produces a low-energy peak (S). The energy distribution curve (shaded area) measured in vacuum exhibits characteristic features related to the different above processes. The vacuum level cuts the low-energy side of the EDC, in particular a considerable portion of the S peak (dashed line).

Partial energy loss during transit through the BBR prior to emission into vacuum broadens the valley contributions towards low energy. But the high-energy thresholds of these contributions will point to the position of the valleys in the bulk. Note that the structures related to the CB valleys can easily be identified since their position is determined by the energy of the valley minimum and does not depend on the excitation energy (provided the photon energy is large enough to populate the considered valley). Prior to emission in vacuum, energy and momentum relaxation near the surface of electrons either photoexcited in the BBR (i.e., at lower energy than in the bulk) or backscattered at the semiconductor/vacuum interface results in the formation of a low-energy contribution (labeled S) which extends down to the bottom of the BBR in the crystal and is cut by the vacuum level in the emitted spectrum. We remark that with near-band-gap excitation (of energy much lower than twice the band gap) photoelectrons do not have enough kinetic energy for exciting the electron-hole pair by impact ionization so that the low-energy peak is not due to secondary electron emission as is usually the case in standard photoemission experiments.

The normalized EDC measured at 5.39 eV excitation energy is shown in Fig. 2 along with its derivative. The EDC (bold line) exhibits a main peak (Γ) with a low-energy shoulder (S) and high-energy contributions (L, B). The different convoluted contributions to the photoemission spectrum are properly resolved when performing a fine analysis of the derivative of the EDC (DEDC) [19]. The DEDC is measured by applying a 60 mV modulation to the cathode potential and detecting the related Faraday cup current modulation with a lock-in amplifier. We clearly observe four contributions. The thermalization in the BBR gives rise to the low-energy positive

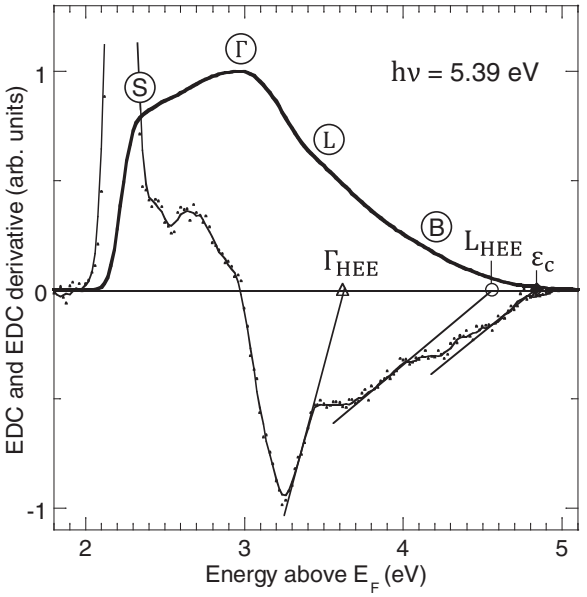


FIG. 2. EDC and corresponding DEDC measured at 5.39 eV excitation energy. The energy scale is referred to the GaN Fermi level. Four different contributions are observed labeled (S), (Γ), (L), and (B). The high-energy extrapolation of the Γ and L contributions is shown on the derivative ($\Gamma_{HEE}$ and $L_{HEE}$) giving an energy separation between Γ and L of $0.92 \pm 0.08$ eV. Due to the overlap of different contributions, $\Gamma_{HEE}$ and $L_{HEE}$ slightly overestimate the bulk positions of the valleys. The high-energy threshold of the spectrum ($\varepsilon_c$) gives the energy of the optical transition final state in the bulk $p$-GaN.

peak. Then, three structures are resolved in the negative part of the DEDC. Two are originating from the electron population accumulated in the Γ and L valleys as will be discussed below. The high-energy threshold of these contributions is evaluated as usual [19], by taking the extrapolation to zero of their high-energy slope ($\Gamma_{HEE}$ and $L_{HEE}$). Finally, the quasiballistic emission contribution appears on the high-energy edge of the DEDC with high-energy threshold $\varepsilon_c$.

Figure 3(a) shows a set of DEDCs recorded for different excitation energies ranging from 3.10 eV to 5.39 eV. For the sake of clarity, the low-energy contribution is not shown. For below-band-gap excitation, electron emission is observed due to electron excitation from the Fermi level near the surface, in agreement with previous observations [26,27]. Beyond the low-energy peak, the spectrum only exhibits a quasiballistic contribution which shifts away from the low-energy contribution and its high-energy threshold lies at $E_F + h\nu$. For excitation energies larger than the band gap of wurtzite GaN $E_g = 3.44$ eV [28], an intense peak is observed with an almost constant energy position. This contribution at fixed energy originates from the accumulation of electrons at the bottom of the Γ valley. On the high-energy side of the Γ peak, the quasiballistic contribution shows up as a shoulder which shifts with increasing $h\nu$. For $h\nu \geqslant 4.63$ eV, this hot-electron structure splits into two contributions: a fixed plateau (labeled L) which corresponds to electron accumulation in an upper conduction valley and a high-energy quasiballistic tail which goes on shifting with $h\nu$.

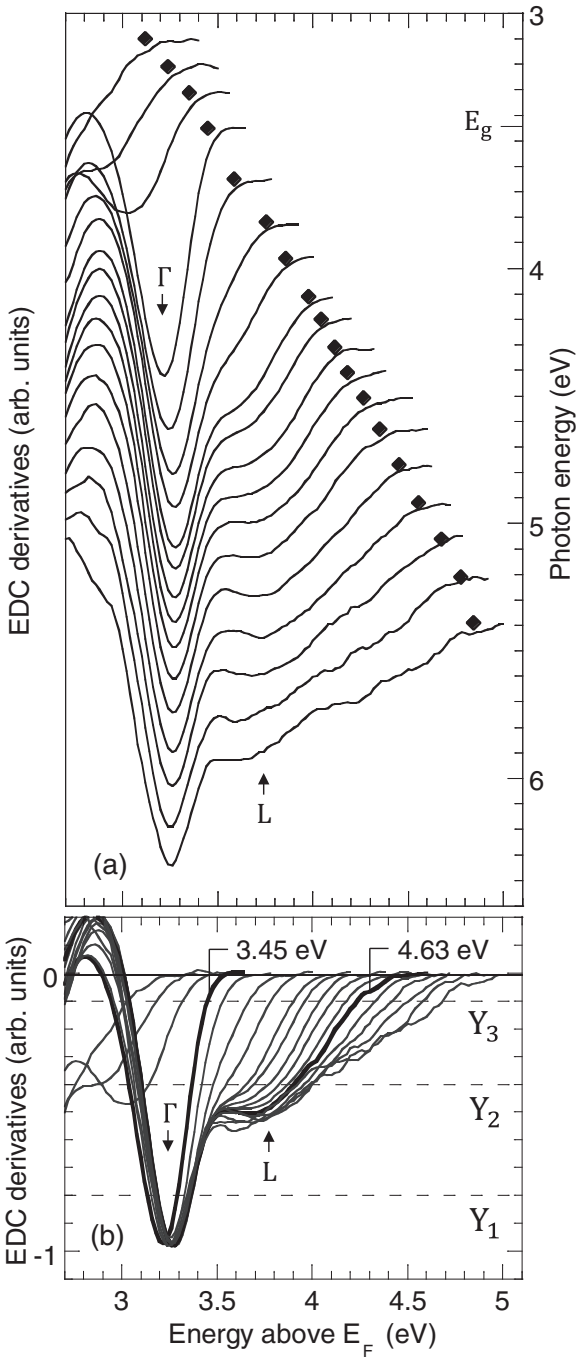


FIG. 3. DEDCs measured for different excitation energies. Curves are normalized to their minimum [31]. Excitation energies: (in eV) 3.10, 3.21, 3.31, 3.45, 3.65, 3.82, 3.96, 4.11, 4.20, 4.31, 4.41, 4.51, 4.63, 4.77, 4.92, 5.06, 5.21, 5.39. (a) The baseline of spectra is shifted according to light energy (right-hand scale). Above $h\nu = 4.63 \pm 0.13$ eV, the position of the L structure is fixed, while the high-energy threshold of the spectra (diamonds) shifts with the excitation energy. (b) Superimposed DEDCs. $Y_1$,$Y_2$, and $Y_3$ are arbitrary ordinates used to track the displacement of different DEDC features as a function of photon energy.

In Fig. 4(a), the extrapolated high-energy thresholds of the structures observed in the DEDCs are plotted as a function of the excitation energy. For below-band-gap excitation, the

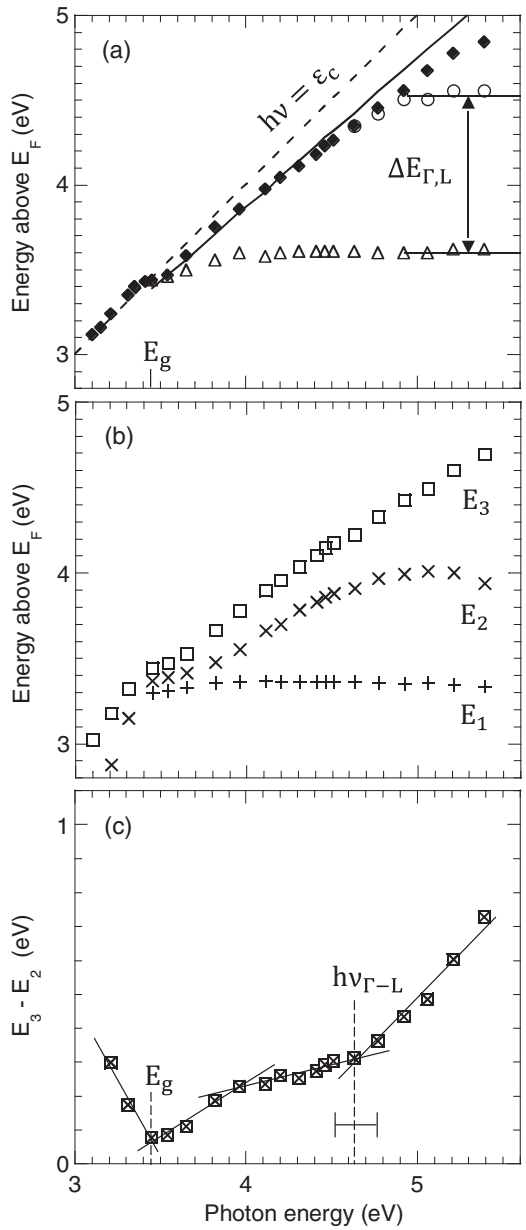


FIG. 4. Energy position above the GaN Fermi level of different features seen in derivative spectra as a function of the excitation energy. (a) High-energy extrapolation of different contributions in DEDCs: Γ peaks ($\Gamma_{HEE}$, triangles), L peaks ($L_{HEE}$, circles), and the high-energy threshold of DEDCs ($\varepsilon_c$, diamonds). The variation of the transition final state energy calculated from the parabolic band approximation ($m_e^* = 0.22m_0$, $m_{hh,z}^* = 1.58m_0$) is plotted as a full line. (b) Variation vs $h\nu$ of $E_1$, $E_2$, and $E_3$, the intercept energies of DEDCs high-energy slopes with $Y_1 = -0.8$, $Y_2 = -0.4$, and $Y_3 = -0.1$ [in arbitrary units; see Fig. 3(b)]. (c) Variation of $E_3 - E_2$ as a function of $h\nu$. The kinks indicated by the vertical dashed lines correspond to the photon energy threshold for populating the Γ and L valleys.

high-energy threshold of the quasiballistic contribution $\varepsilon_c$ closely follows the dashed line of unity slope, indicating that optical transitions occur in the BBR with initial states at $E_F$. For above-band-gap excitation, the variation of $\varepsilon_c$ with $h\nu$ deviates from the line of unity slope because it corresponds to the final state of direct interband transitions from the heavy-hole band for which the excess energy, $h\nu - E_g$, is shared among electrons and holes according to their respective effective masses. The full line represents the calculated variation of the final state for optical transitions from the heavy-hole band, assuming parabolic bands with effective masses $m_e^* = 0.22m_0$ for electrons and $m_{hh,z}^* = 1.58m_0$ for holes. Taking $E_F = 60$ meV above the valence band maximum, this curve fits well with the experimental variation of $\varepsilon_c$ up to $h\nu \sim 4.5$ eV. The slight deviation between calculation and experimental values observed at higher excitation energy is due to the nonparabolicity of the bands away from the Γ point [29,30]. The extrapolated high-energy thresholds of the Γ and L contributions, $\Gamma_{HEE}$ and $L_{HEE}$, exhibit fixed positions from which we deduce a Γ-L separation of $\Delta E_{\Gamma,L} = 0.92 \pm 0.08$ eV, with an uncertainty that takes into account the spectrometer resolution. Note that, due to the overlap of the different contributions, the extrapolated high-energy thresholds slightly overestimate the absolute bulk energy position of Γ and L (for instance $\Gamma_{HEE}$ lies at $3.61 \pm 0.08$ eV above $E_F$, while Γ is expected at 3.38 eV above $E_F$). A similar effect was also observed in GaAs at room temperature [19]. However, this should not significantly affect the measurement of the relative position of Γ and L.

In order to confirm this assumption we use a data analysis procedure which allows to independently determine the optical threshold for populating the L valley by phonon-assisted intervalley transfer. From the value of this threshold, we straightforwardly deduce the energy position of the L-valley minimum. This procedure consists in tracking the intercepts of the high-energy slope of DEDCs with three arbitrary ordinates, $Y_1$, $Y_2$, and $Y_3$, as shown in Fig. 3(b). The variation of the intercept energies $E_1$, $E_2$, and $E_3$ versus photon energy is plotted in Fig. 4(b). The intercept energy $E_1$ remains constant since $Y_1$ only crosses the Γ structure for $h\nu \geqslant E_g$, while the intercept energy $E_3$ constantly increases with $h\nu$ since it corresponds to quasiballistic electron emission. The intercept energy $E_2$ initially increases with photon energy similarly to $E_3$, i.e., to the quasiballistic contribution. It then reaches a stable value indicating electron transfer and accumulation in the L valley. The difference between $E_3$ and $E_2$ is plotted in Fig. 4(c) as a function of $h\nu$. Two kinks are observed at $h\nu =$ 3.45 eV and 4.63 eV corresponding to the excitation energies where the intercept energy $E_2$ deviates from the variation of $E_3$, which is characteristic of the ballistic electron behavior. The first kink at $h\nu = E_g$ is due to the transition from below to above band-gap excitation and corresponds to electron accumulation in Γ. The second kink at $h\nu = 4.63 \pm 0.13$ eV corresponds to electron transfer and accumulation in the L valley and directly gives the optical threshold $h\nu_{\Gamma\text{-}L}$ for the activation of the Γ-L intervalley transfer. The measured value of $h\nu_{\Gamma\text{-}L}$, close to the one of $4.51 \pm 0.05$ eV determined by Wu *et al.* [8], gives an independent determination of the energy position of the L valley. Using the parabolic approximation we can calculate the value of conduction final state energy for $h\nu = 4.63$ eV. Then, taking the intervalley phonon energy as 92 meV, we obtain $0.95 \pm 0.13$ eV for the position of L above the CB minimum. We can refine this estimation by taking into account nonparabolicity. We indeed measure the highest

possible optical transition final state $\varepsilon_c$. At $h\nu = 4.63$ eV we obtain $\varepsilon_c = 4.35$ eV above $E_F$, that is 0.97 eV above Γ. Considering the emission of an intervalley phonon of energy 92 meV, we obtain $0.88 \pm 0.13$ eV for the position of the L valley above Γ, which is consistent with the value of $\Delta E_{\Gamma,L}$ that we obtained from the extrapolation of the Γ and L structures. Note that this procedure is quite robust and the result is unchanged when choosing other values of $Y_1$, $Y_2$, $Y_3$ within a reasonable range [typically ±0.05 in the scale of Fig. 3(b)].

In conclusion, we have carried out a photoemission spectroscopy study of wurtzite *p*-GaN to determine important CB parameters. With a fine tuning of the excitation energy, the derivatives of the photoelectron EDCs exhibit two structures with fixed energy positions that are unambiguously related to the emission of electrons accumulated in two different CB valleys, namely the Γ valley and the first satellite valley that we assume to be L. From these data, we obtain two independent determinations for the Γ-L separation: $0.92 \pm 0.08$ eV is directly measured as the distance between the high-energy extrapolation of the Γ and L structures, while $0.88 \pm 0.13$ eV is deduced from the excitation threshold at which the fixed L structure shows up. The above direct consistent measurements that we obtained allow us to establish the L-valley position in wurtzite GaN at $\Delta E_{\Gamma,L} = 0.90 \pm 0.08$ eV above the CB minimum. This value contrasts with the much higher theoretical predictions provided by *ab initio* calculations and confirms previous indirect experimental estimates.

The work at UCSB is supported by the Center for Energy Efficient Materials (CEEM), an Energy Frontier Research Center funded by the U.S. Department of Energy, Office of Science, Office of Basic Energy Sciences, under Award No. DE-SC0001009.

[1] Y. Narukawa, M. Ichikawa, D. Sanga, M. Sano, and T. Mukai, J. Phys. D **43**, 354002 (2010).
[2] A. Dyson and B. K. Ridley, J. Appl. Phys. **104**, 113709 (2008).
[3] R. Brazis and R. Raguotis, Appl. Phys. Lett. **85**, 609 (2004).
[4] E. G. Brazel, M. A. Chin, V. Narayanamurti, D. Kapolnek, E. J. Tarsa, and S. P. DenBaars, Appl. Phys. Lett. **70**, 330 (1997).
[5] N. Nepal, K. B. Nam, J. Li, M. L. Nakarmi, J. Y. Lin, and H. X. Jiang, Appl. Phys. Lett. **88**, 261919 (2006).
[6] M. Semenenko, O. Yilmazoglu, H. L. Hartnagel, and D. Pavlidis, J. Appl. Phys. **109**, 023703 (2011).
[7] C. K. Sun, Y. L. Huang, S. Keller, U. K. Mishra, and S. P. DenBaars, Phys. Rev. B **59**, 13535 (1999).
[8] S. Wu, P. Geiser, J. Jun, J. Karpinski, D. Wang, and R. Sobolewski, J. Appl. Phys. **101**, 043701 (2007).
[9] A. M. Witowski, K. Pakula, J. M. Baranowski, M. L. Sadowski, and P. Wyder, Appl. Phys. Lett. **75**, 4154 (1999).
[10] M. Drechsler, D. Hofmann, B. Meyer, T. Detchprohm, H. Amano, and I. Akasaki, Jpn. J. Appl. Phys. **34**, L1178 (1995).
[11] B. Santic, Semicond. Sci. Technol. **18**, 219 (2003).
[12] J. Cao and X. Lei, Eur. Phys. J. B **7**, 79 (1999).
[13] J. Iveland, L. Martinelli, J. Peretti, J. S. Speck, and C. Weisbuch, Phys. Rev. Lett. **110**, 177406 (2013).
[14] R. Wang, P. Ruden, J. Kolnik, I. Oguzman, and K. Brennan, J. Phys. Chem. Solids **58**, 913 (1997).
[15] In theoretical band structures the first satellite valley is called U, lying between the L and M points of the Brillouin zone. Typically experiments do not have a determination in $k$ space and generally refer to it as the L valley.
[16] M. Goano, E. Bellotti, E. Ghillino, G. Ghione, and K. F. Brennan, J. Appl. Phys. **88**, 6467 (2000).
[17] K. T. Delaney, P. Rinke, and C. G. Van de Walle, Appl. Phys. Lett. **94**, 191109 (2009).
[18] L. C. de Carvalho, A. Schleife, and F. Bechstedt, Phys. Rev. B **84**, 195105 (2011).
[19] H.-J. Drouhin, C. Hermann, and G. Lampel, Phys. Rev. B **31**, 3859 (1985).
[20] J. Peretti, H.-J. Drouhin, D. Paget, and A. Mircéa, Phys. Rev. B **44**, 7999 (1991).
[21] R. C. Eden, J. L. Moll, and W. E. Spicer, Phys. Rev. Lett. **18**, 597 (1967).
[22] J. F. Muth, J. H. Lee, I. K. Shmagin, R. M. Kolbas, H. C. Casey, B. P. Keller, U. K. Mishra, and S. P. DenBaars, Appl. Phys. Lett. **71**, 2572 (1997).
[23] O. Tereshchenko, G. Shaibler, A. Yaroshevich, S. Shevelev, A. Terekhov, V. Lundin, E. Zavarin, and A. Besyul'kin, Phys. Solid State **46**, 1949 (2004).
[24] J. Peretti, H.-J. Drouhin, and D. Paget, Phys. Rev. B **47**, 3603 (1993).
[25] H.-J. Drouhin and M. Eminyan, Rev. Sci. Instrum. **57**, 1052 (1986).
[26] A. Pakhnevich, V. Bakin, A. Yaz'kov, G. Shaibler, S. Shevelev, O. Tereshchenko, A. Yaroshevich, and A. Terekhov, J. Exp. Theor. Phys. Lett. **79**, 479 (2004).
[27] A. Pakhnevich, V. Bakin, G. Shabler, and A. Terekhov, Phys. Solid State **49**, 2070 (2007).
[28] B. Monemar, Phys. Rev. B **10**, 676 (1974).
[29] P. A. Shields, R. J. Nicholas, F. M. Peeters, B. Beaumont, and P. Gibart, Phys. Rev. B **64**, 081203 (2001).
[30] S. Syed, J. B. Heroux, Y. J. Wang, M. J. Manfra, R. J. Molnar, and H. L. Stormer, Appl. Phys. Lett. **83**, 4553 (2003).
[31] Due to the low PE quantum yield at below-band-gap excitation, for best comparison, spectra measured at $h\nu < E_g$ have been normalized to the maximum of the DEDC measured at $h\nu = 3.45$ eV.